

# Micro-LED Nanosecond Pulsed Structured Light Sources with 405 nm – 510 nm Wavelength

J.A. Gray<sup>1</sup>, J.J.D McKendry<sup>1</sup>, J.H. Herrnsdorff<sup>1</sup>, M.J. Strain<sup>1</sup>, R.K. Henderson<sup>2</sup> and M.D. Dawson<sup>1</sup>

1. Institute of Photonics, Department of Physics, University of Strathclyde, 99 George St, G1 1RD, Glasgow, U.K.

2. School of Engineering, University of Edinburgh, King’s Buildings, Alexander Crum Brown Road, EH9 3FF, Edinburgh, U.K.  
*Johnathan.gray.2020@uni.strath.ac.uk*

**Narrow-pulse visible light sources are crucial to time-resolved imaging. We present 16k-element MicroLED arrays spanning the visible region allowed by InGaN/GaN, achieving 3 ns pulses at up to 100 MHz repetition rate with programmable illumination patterns.**

**Keywords—** *MicroLEDs, LiFi, Gallium Nitride, FLIM, TCSPC.*

## I. INTRODUCTION

Digital light projection with structured illumination sources has enabled a vast range of novel techniques in recent years, from visible light communications (LiFi) [1] to fluorescent lifetime imaging microscopy (FLIM), relying on pulsed illumination at specific wavelengths [2]. The “Megaprojector”, a 16k element array of 30 x 30  $\mu\text{m}$  GaN micro-light-emitting-diodes (micro-LEDs), is capable of pulsing patterns at up to  $\sim 4$  ns and transmitting  $>5$  Gbps data rates [3].

While the initial report on this technology was confined to a wavelength of 450 nm, we extend this work here to the entire range supported by conventional InGaN/GaN LED epitaxial structures. Two 128 x 128 MicroLED arrays emitting 405 nm and 510 nm have had their pulse-capabilities characterised and are reported here. Green and violet emission is of key importance to FLIM and time-correlated single-photon counting (TCSPC), which often use fluorophores with peak absorption wavelengths in this range [4].

## II. EXPERIMENTAL METHOD

### A. Pulse Characterisation

The Megaprojector was focused onto a high bandwidth photomultiplier tube (PMT) to collect the optical pulses. The PULSE output providing an electrical signal from the FPGA to the CMOS driver was monitored with an oscilloscope, along with the PMT output as shown in Fig. 1.

The chips were driven by a 5 ns electrical pulse, the number of active pixels in the illumination pattern was varied in the range 10-1000 pixels, and the repetition rate was in the range 10-100 MHz. Oscilloscope data was read into MATLAB where the full width half maximum (FWHM) of the received optical pulses was found.

### B. Optical Pulse Energy and Power Per Pixel

A Thorlabs optical power metre was placed on top of each Megaprojector chip while varying numbers of MicroLEDs were pulsed to determine the optical power vs. brightness for

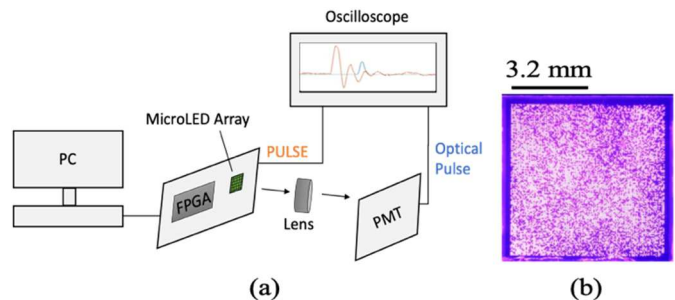


Fig. 1. (a) Schematic of set-up to collect optical pulses from the Megaprojector and (b) an optical micrograph of the violet device, measuring 6.4 mm across.

representative pixels, and how total pulse energy and pulse energy per pixel varied with number of pixels displayed.

### C. Intracolumn and Intrarow Delay

The row and column with highest number of working MicroLEDs was found for the green and violet device. The LEDs within the best row/column were pulsed individually and the delay between the driving electronic PULSE signal and the received optical pulse was used to determine the timing delay between pixels within each row/column.

## III. RESULTS

The devices characterised here are of varying pixel yield due to their research-prototype nature, with the lowest being the green chip and highest a 450 nm blue array of  $>98\%$  yield. The bonding process between the CMOS and micro-LEDs gives rise to the varying yield, rather than the components themselves.

A representative single micro-LED within the array displayed 8.32  $\mu\text{W}$  and 4.96  $\mu\text{W}$  at maximum brightness (87  $\mu\text{A}$  current) for the violet and green device respectively, as in Fig. 4. The lower green LED output power is due to the known efficiency droop from increasing Indium content [5]. Both devices showed a clear linear relationship between the width of the input electrical pulse and the output optical pulse, as seen with previous devices [3].

The optical FWHM is  $\sim 3$  ns for the violet chip and increased with number of active pixels until reaching a threshold, past which individual pixels receive less current until switching off entirely, as shown in Fig. 3. The green device achieved 4 ns pulses at 10 MHz repetition rate and 5 ns at up to 100 MHz.

This work was carried out under EPSRC grant EP/T517938/1. Data can be found at <https://doi.org/10.15129/75816126-1c60-4296-8efe-b88bafd4f892>.

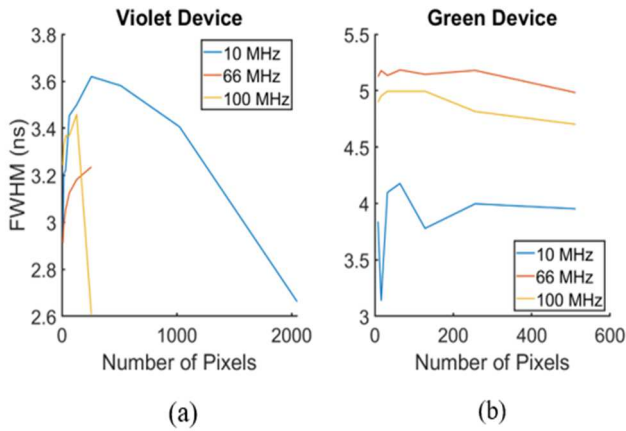


Fig. 2. (a) FWHM vs number of pixels for the 405 nm and (b) 510 nm array as a function of pulse repetition rate.

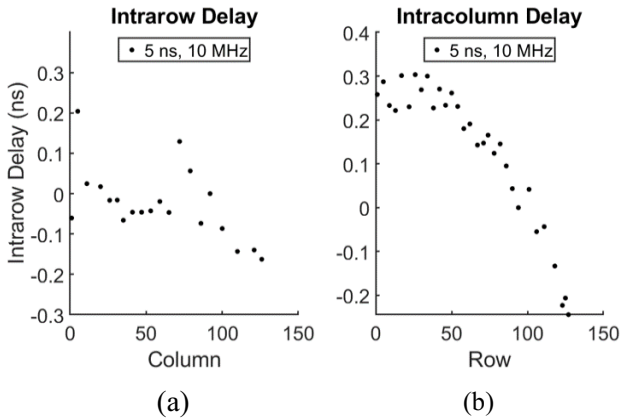


Fig. 3. (a) Intrarow and (b) intracolumn delay for the violet array.

Fig. 3 demonstrates the relative delay between input electrical pulse from the FPGA driver to pixels in varying rows, due to layout of the CMOS driver chip. There is no significant trend in delay between columns, consistent with the chip layout and findings with previous blue arrays [1]. Importantly, the overall delay is less than 1 ns, which crucially enables complex illumination patterns to pulse in a synchronized fashion with  $<5$  ns time resolution.

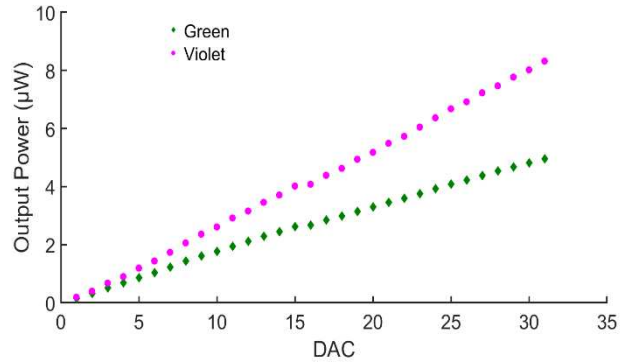


Fig. 4. Output power vs. DAC for a representative MicroLED on either device.

#### IV. CONCLUSION

We have demonstrated few-nanosecond pulses at up to 100 MHz repetition rate using programmable illumination patterns with up to 1000 active pixels within 16k-element InGaN/GaN MicroLED arrays spanning the 405 nm – 510 nm spectral range. These devices could act as the light source in FLIM experiments, where narrow pulses at high repetition rates are crucial and require photons in the visible region due to the chemicals used [2]. There are also possible applications in communications with thousands of individual transmitters available at different wavelengths.

#### REFERENCES

- [1] A. D. Griffiths, J. Hermsdorf, J. J. D. McKendry, M. J. Strain, & M. D. Dawson (2020). Gallium nitride micro-light-emitting diode structured light sources for multi-modal optical wireless communications systems. *Philosophical Transactions of the Royal Society A: Mathematical, Physical and Engineering Sciences*, 378(2169), 20190185. <https://doi.org/10.1098/rsta.2019.0185>.
- [2] B. R. Rae, C. Griffin, J. McKendry, J. M. Girkin, H. X. Zhang, E. Gu, D. Renshaw, E. Charbon, M. D. Dawson, & R. K. Henderson (2008). CMOS driven micro-pixel LEDs integrated with single photon avalanche diodes for time resolved fluorescence measurements. *Journal of Physics D: Applied Physics*, 41(9), 094011. <https://doi.org/10.1088/0022-3727/41/9/094011>.
- [3] N. Bani Hassan, F. Dehkoda, E. Xie, J. Hermsdorf, M. J. Strain, R. Henderson, & M. D. Dawson (2022). Ultrahigh frame rate digital light projector using chip-scale LED-on-CMOS technology. *Photonics Research*, 10(10), 2434. <https://doi.org/10.1364/PRJ.455574>.
- [4] J. R. Lakowicz (Ed.). (2006). *Principles of Fluorescence Spectroscopy*. Springer US. <https://doi.org/10.1007/978-0-387-46312-4>.
- [5] G. Verzellesi, D. Saguatti, M. Meneghini, F. Bertazzi, M. Goano, G. Meneghesso, & E. Zanoni (2013). Efficiency droop in InGaN/GaN blue light-emitting diodes: Physical mechanisms and remedies. *Journal of Applied Physics*, 114(7), 071101. <https://doi.org/10.1063/1.4816434>.